Modeling Epidemic Spreading in Complex Networks: Concurrency and Traffic

Sandro Meloni, Alex Arenas, Sergio Gómez, Javier Borge-Holthoefer and Yamir Moreno

Abstract The study of complex networks sheds light on the relation between the structure and function of complex systems. One remarkable result is the absence of an epidemic threshold in infinite-size scale-free networks, which implies that any infection will perpetually propagate regardless of the spreading rate. However, real-world networks are finite and experience indicates that infections do have a finite lifetime. In this chapter we will provide with two new approaches to cope with the problem of concurrency and traffic in the spread of epidemics. We show that the epidemic incidence is shaped by contact flow or traffic conditions. Contrary to the classical assumption that infections are transmitted as a diffusive process from nodes to all neighbors, we instead consider the scenario in which epidemic pathways are defined and driven by flows. Extensive numerical simulations and theoretical

Sandro Meloni
Department of Informatics and Automation, University of Rome "Roma Tre", Via della Vasca Navale, 79 Rome 00146, Italy

Alex Arenas
Departament d'Enginyeria Informàtica i Matemàtiques, Universitat Rovira i Virgili, 43007 Tarragona, Spain
Instituto de Biocomputación y Física de Sistemas Complejos (BIFI), Universidad de Zaragoza, Corona de Aragón 42, 50009 Zaragoza, Spain

Sergio Gómez
Departament d'Enginyeria Informàtica i Matemàtiques, Universitat Rovira i Virgili, 43007 Tarragona, Spain

Javier Borge-Holthoefer
Departament d'Enginyeria Informàtica i Matemàtiques, Universitat Rovira i Virgili, 43007 Tarragona, Spain
Instituto de Biocomputación y Física de Sistemas Complejos (BIFI), Universidad de Zaragoza, Corona de Aragón 42, 50009 Zaragoza, Spain

Yamir Moreno
Instituto de Biocomputación y Física de Sistemas Complejos (BIFI), Universidad de Zaragoza, Corona de Aragón 42, 50009 Zaragoza, Spain
Departamento de Física Teórica, Universidad de Zaragoza, 50009 Zaragoza, Spain

predictions show that whether a threshold exists or not depends directly on contact flow conditions. Two extreme cases are identified. In the case of low traffic, an epidemic threshold shows up, while for very intense flow, no epidemic threshold appears. In this way, the classical mean-field theory for epidemic spreading in scale free networks is recovered as a particular case of the proposed approach. Our results explain why some infections persist with low prevalence in scale-free networks, and provide a novel conceptual framework to understand dynamical processes on complex networks.

1 Introduction

The problem of modeling how diseases spread among individuals has been intensively studied for many years [31, 2, 20, 39]. The development of mathematical models to guide our understanding of the disease dynamics has allowed to address important issues such as immunization and vaccination policies [2, 32, 22]. Physicist's approaches to problems in epidemiology involve statistical physics, the theory of phase transitions and critical phenomena [53], which have been extremely helpful to grasp the macroscopic behavior of epidemic outbreaks [45, 46, 34, 38, 41, 4, 24, 37, 15]. The main artifice of this success has been the Mean-Field (MF) approximation, where local homogeneities of the ensemble are used to average the system, reducing degrees of freedom. It consists of coarse-grained vertices within degree classes and considers that all nodes in a degree class have the same dynamical properties; the approach also assumes that fluctuations can be neglected.

The study of complex networks [42, 6, 21] has provided new grounds to the understanding of contagion dynamics. Particularly important in nature are scale-free (SF) networks, whose degree distribution follows a power law $P(k) \sim k^{-\gamma}$ for the number of connections, k, an individual has. SF networks include patterns of sexual contacts [33], the Internet [47], as well as other social, technological and biological networks [10]. SF networks [6, 21, 3] are characterized by the presence of hubs, which are responsible for several striking properties for the propagation of information, rumors or infections [45, 34, 38, 41, 4, 24]. The HMF approach analytically predicts predicts the critical rate β_c at which the disease spreads, i.e. the epidemic threshold.

Theoretical modeling of how diseases spread in complex networks is largely based on the assumption that the propagation is driven by reaction processes, in the sense that the transmission occurs from every infected through all its neighbors at each time step, producing a diffusion of the epidemics on the network. However, this approach overlooks the notion that the network substrate is a fixed snapshot of all the possible connections between nodes, which does not imply that all nodes are concurrently active [26]. Many networks observed in nature [6, 21], including those in society, biology and technology, have nodes that temporally interact only with a subset of its neighbors [1, 43]. For instance, hub proteins do not always interact with all their neighbor proteins at the same time [30], just as individuals in a social net-

work [33] do not interact simultaneously with all of their acquaintances. Likewise, Internet connections being utilized at a given time depends on the specific traffic and routing protocols. Given that transport is one of the most common functions of networked systems, a proper consideration of this issue will irreparably affect how a given dynamical process evolves.

In this chapter, we present a theoretical framework for contact-based spreading of diseases in complex networks. This formulation, Microscopic Markov-Chain Approach (MMCA), is based on probabilistic discrete-time Markov chains, generalizes existing HMF approaches and applies to weighted and unweighted complex networks [26]. Within this context, in addition to capturing the global dynamics of the different contact models and its associated critical behavior, it is now possible to quantify the *microscopic dynamics* at the individual level by computing the probability that any node is infected in the asymptotic regime. MC simulations corroborate that the formalism here introduced reproduces correctly the *whole* phase diagram for model and real-world networks. Moreover, we capitalize on this approach to address how the spreading dynamics depends on the number of contacts actually used by a node to propagate the disease.

After that, we introduce a theoretical approach to investigate the outcome of an epidemic spreading process driven by transport instead of reaction events [37]. To this end, we analyze a paradigmatic abstraction of epidemic contagion, the so-called Susceptible-Infected-Susceptible (SIS) model [40], which assumes that contagion occurs through the eventual contact or transmission between connected partners that are using their connections at the time of propagation. This is achieved by considering a quantized interaction at each time step. Mathematically, we set up the model in a flow scenario where contagion is carried by interaction packets traveling across the network. We consider two possible scenarios that encompass most of real traffic situations: i) unbounded delivery rate, and ii) bounded delivery rate, of packets per unit time. We derive the equation governing the critical threshold for epidemic spreading in SF networks, which embeds, as a particular case, previous theoretical findings. For unbounded delivery rate, it is shown that the epidemic threshold decreases in *finite* SF networks when traffic flow increases. In the bounded case, nodes accumulate packets at their queues when traffic flow overcomes the maximal delivery rate, i.e. when congestion arises. From this moment on, the results show that both the epidemic threshold and the infection prevalence are bounded due to congestion.

2 Microscopic Markov-Chain Approach to disease spreading

The critical properties of an epidemic outbreak in SF networks can be addressed using the heterogeneous MF (HMF) prescription [45, 46, 34, 38, 41, 4, 24, 37]. It consists of coarse-grained vertices within degree classes and considers that all nodes in a degree class have the same dynamical properties; the approach also assumes that fluctuations can be neglected. Specifically, if β is the rate (probability per unit time)

at which the disease spreads, it follows that the epidemic threshold in uncorrelated SF networks is given [45] by $\beta_c = \langle k \rangle / \langle k^2 \rangle$, leading to $\beta_c \to 0$ as $N \to \infty$ when $2 < \gamma \leq 3$.

MF approaches are extremely useful to assess the critical properties of epidemic models, however they are not designed to give information about the probability of individual nodes but about classes of nodes. Then, questions concerning the probability that a given node be infected are not well posed in this framework. To obtain more details at the individual level of description, one has to rely on Monte Carlo (MC) simulations, which have also been used to validate the results obtained using MF methods. Restricting the scope of epidemiological models to those based in two states [31, 20, 39] −susceptible (S) and infected (I)−, the current theory concentrates on two specific situations, the contact process [35, 11, 29, 12, 13, 7] (CP) and the reactive process [23, 14, 18] (RP). A CP stands for a dynamical process that involves an individual stochastic contagion per infected node per unit time, while in the RP there are as many stochastic contagions per unit time as neighbors a node has. This latter process underlies the abstraction of the susceptible-infected-susceptible (SIS) model [31, 20, 39]. However, in real situations, the number of stochastic contacts per unit time is surely a variable of the problem itself [26]. In this first part of the chapter we develop a microscopic model, based on Markov-Chains, to cope with the concurrency problem in the spreading of epidemics.

2.1 Contact-based epidemic spreading models

Let us suppose we have a complex network, undirected or directed, made up of N nodes, whose connections are represented by the entries $\{a_{ij}\}$ of an N-by-N adjacency matrix $\mathbf{A}$, where $a_{ij} \in \{0, 1\}$. Unlike standard HMF approaches, our formalism allows the analysis of weighted networks, thus we denote by $\{w_{ij}\}$ the non-negative weights ($w_{ij} \geq 0$) of the connections between nodes, being $w_i = \sum_j w_{ij}$ the total output strength [5] of node i. The above quantities completely define the structure of the underlying graph. The dynamics we consider is a discrete two-state contact-based process, where every node is either in a susceptible (S) or infected (I) state. Each node of the network represents an individual (or a place, a city, an airport, etc.) and each edge is a connection along which the infection spreads. At each time step, an infected node makes a number λ of trials to transmit the disease to its neighbors with probability β per unit time, and then has a probability μ of recovering to the susceptible state. This forms a Markov chain where the probability of a node being infected depends only on the last time step, hence the name Microscopic Markov-Chain Approach (MMCA). After some transient time, the previous dynamics sets the system into a stationary state in which the average density of infected individuals, ρ, defines the prevalence of the disease.

We are interested in the probability $p_i(t)$ that any given node i is infected at time step t. We denote by r_{ij} the probability that a node i is in contact with a node j, defining a matrix $\mathbf{R}$. These entries represent the probabilities that existing links in

the network are used to transmit the infection. If i and j are not connected, then $r_{ij} = 0$. With these definitions, the discrete-time version of the evolution of the probability of infection of any node i reads

$$p_i(t+1) = (1 - q_i(t))(1 - p_i(t)) + (1 - \mu)p_i(t) + \mu(1 - q_i(t))p_i(t), \qquad (1)$$

where $q_i(t)$ is the probability of node i not being infected by any neighbor at time t,

$$q_i(t) = \prod_{j=1}^{N}(1 - \beta r_{ji}p_j(t)). \qquad (2)$$

The first term on the right hand side of eq. (1) is the probability that node i is susceptible $(1 - p_i(t))$ and is infected $(1 - q_i(t))$ by at least a neighbor. The second term stands for the probability that node i is infected at time t and does not recover, and finally the last term takes into account the probability that an infected node recovers $(\mu p_i(t))$ but is re-infected by at least a neighbor $(1 - q_i(t))$. Within this formulation, we are assuming the most general situation in which recovery and infection occur on the same time scales, allowing then reinfection of individuals during a discrete time window (for instance, one MC step). This formulation generalizes previous approximations where one time step reinfections can not occur.

The formulation so far relies on the assumption that the probabilities of being infected p_i are independent random variables. This hypothesis turns out to be valid in the vast majority of complex networks because the inherent topological disorder makes dynamical correlations not persistent. The dynamical system (1, 2) corresponds to a family of possible models, parameterized by the explicit form of the contact probabilities r_{ij}. Without loss of generality, it is instructive to think of these probabilities as the transition probabilities of random walkers on the network. The general case is represented by λ_i random walkers leaving node i at each time step:

$$r_{ij} = 1 - \left(1 - \frac{w_{ij}}{w_i}\right)^{\lambda_i}. \qquad (3)$$

The Contact Process (CP) corresponds to a model dynamics of one contact per unit time, $\lambda_i = 1$, $\forall i$ in eq. (3) thus $r_{ij} = w_{ij}/w_i$[1]. In the Reactive Process (RP) all neighbors are contacted, which corresponds, in this description, to set the limit $\lambda_i \to \infty$, $\forall i$ resulting on $r_{ij} = a_{ij}$ regardless of whether the network is weighted or not. Other prescriptions for λ_i conform the spectrum of models that can be obtained using this unified framework. The phase diagram of every model is simply obtained solving the system formed by eq. (1) for $i = 1, \ldots, N$ at the stationary state,

$$p_i = (1 - q_i) + (1 - \mu)p_i q_i, \qquad (4)$$

---

[1] Strictly speaking, when $\lambda = 1$, our model is not exactly the standard CP, since in that case reinfections are not considered. However, we will refer to it as a CP since only one neighbor is contacted at each time step and the critical points of both variants are the same.

$$q_i = \prod_{j=1}^{N}(1 - \beta r_{ji}p_j).$$ (5)

This equation has always the trivial solution $p_i = 0, \forall i = 1, \ldots, N$. Other non-trivial solutions are reflected as non zero fixed points of eqs. (4) and (5), and can be easily computed numerically by iteration. The macroscopic order parameter is given by the expected fraction of infected nodes ρ, computed as

$$\rho = \frac{1}{N}\sum_{i=1}^{N}p_i.$$ (6)

2.2 Numerical results

To show the validity of the MMCA model here discussed, we have performed MC simulations on different SF networks for RP. In Figure 1 the phase diagram of the system obtained by MC simulations is compared with the numerical solution of eqs. (4) and (5). To model the epidemic dynamics on the described topologies we incorporate a SIS model in which, at each time step, each node can be susceptible or infected. Each simulation starts with a fraction ρ_0 of randomly chosen infected individuals ($\rho_0 = 0.05$ in our simulations), and time is discretized in time-steps. At each time step an infected node i infects with the same probability β all its neighbors and recovers at a rate μ. The simulation runs until a stationary state for the density of susceptible individuals, $\rho(t)$ is reached. The agreement between both curves is matchless. Moreover, the formalism also captures the microscopic dynamics as given by the p_i's, see the inset of Fig. 1. While the computational cost of the MC simulations is considerably large, the numerical solution of the fix point eqs. (4) and (5), by iteration, is fast and accurate.

In Fig. 2 we analyze our formalism on top of the airports network data set, composed of passenger flights operating in the time period November 1, 2000, to October 31, 2001 compiled by OAG Worldwide (Downers Grove, IL) and analyzed previously by Prof. Amaral's group [28]. It consists of 3618 nodes (airports) and 14142 links, we used the weighted network in our analysis. Airports corresponding to a metropolitan area have been collapsed into one node in the original database. We show the density of infected individuals ρ as a function of β for different values of λ. Both the critical points and the shape of the $\rho - \beta$ phase diagrams greatly change at varying the number of stochastic contacts (λ). We observe a moderate disease prevalence in the case of small values of λ, even for large values of the spreading rate β. In contrast, when the number of trials is of order 10^3 the situation is akin to a RP.

Finally, we compare the results of the formalism for different random scale-free networks satisfying $P(k) \sim k^{-\gamma}$, which have been generated using the configuration model [6, 21] with a fixed size of $N = 10^4$ nodes. Fig. 3 shows the phase diagram for $\mu = 1$ and several values of the exponent γ, both below and above $\gamma = 3$. Symbols
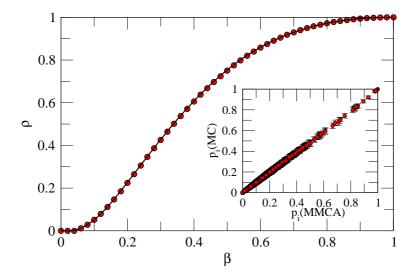
Fig. 1 Average fraction of infected nodes ρ as a function of the infection rate β for $N = 10^4$. Lines stand for the MMCA solutions (with $\lambda = \infty$) and symbols correspond to MC simulations of the SIS model on top of random scale-free networks with $\gamma = 2.7$ (error bars are smaller than the size of the symbol). In the inset, scatter plot for the probability that a node is infected using results of MC simulations (the y-axis) and the solutions (x-axis) of eqs. (4) and (5). Both results have been obtained for $\mu = 1$, the inset is for $\beta = 0.1$. After [26].

correspond to MC simulations, whereas dotted lines represent the results obtained using the analytical approximation. As it can be seen, the agreement between both methods is remarkable, even for values of $\gamma < 2.5$ where structural changes are extremely relevant [51]. On the other hand, one may explore the dependency with the system size while fixing the degree distribution exponent γ. This is what is shown in Fig. 4, where we have depicted the phase diagram for networks with $\gamma = 2.7$ for several system sizes ranging from $N = 500$ to $N = 10^5$. Except for $N = 500$, where MC results have a large standard deviation close to the critical point, the agreement is again excellent in the whole range of β values.

2.3 Epidemic Threshold

Let us now assume the existence of a critical point β_c for fixed values of μ and λ_i such that $\rho = 0$ if $\beta < \beta_c$ and $\rho > 0$ when $\beta > \beta_c$. The calculation of this critical point is performed by considering that when $\beta \to \beta_c$, the probabilities $p_i \approx \varepsilon_i$, where $0 \le \varepsilon_i \ll 1$, and then after substitution in eq. (2) one gets
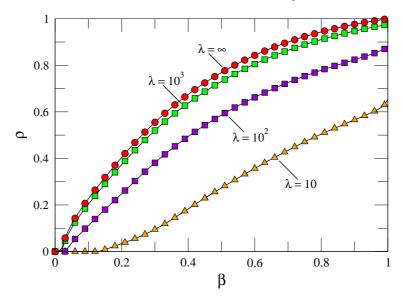
Fig. 2 Density of infected individuals ρ as a function of β for different values of λ in the air transportation network [28]. The smallest epidemic threshold and largest incidence is obtained for the RP, in which the matrix R corresponds to the adjacency matrix. This implies that the SIS on unweighted networks is a worst case scenario for the epidemic spreading in real weighted networks. ρ is calculated according to eq. (6) once the p_i's are obtained, μ is set to 1. After [26].

$$q_i \approx 1 - \beta \sum_{j=1}^{N} r_{ji}\varepsilon_j . \tag{7}$$

Inserting eq. (7) in eq. (4), and neglecting second order terms in ε we get

$$\sum_{j=1}^{N} \left(r_{ji} - \frac{\mu}{\beta}\delta_{ji} \right) \varepsilon_j = 0, \qquad \forall i = 1, \ldots, N, \tag{8}$$

where δ_{ij} stands for the Kronecker delta. The system (8) has non trivial solutions if and only if μ/β is an eigenvalue of the matrix **R**. Since we are looking for the onset of the epidemic, the lowest value of β satisfying (8) is

$$\beta_c = \frac{\mu}{\Lambda_{\max}}, \tag{9}$$

where $\Lambda_{\max}$ is the largest eigenvalue of the matrix **R**. Equation (9) defines the epidemic threshold of the disease spreading process.

With the previous development it is worth analyzing the two limiting cases of CP and RP above. In the first case, one must take into account that the matrix **R** is a transition matrix whose maximum eigenvalue is always $\Lambda_{\max} = 1$. Thus the trivial result that the only non-zero solution corresponds to $\beta_c = \mu$. For the RP corresponding to
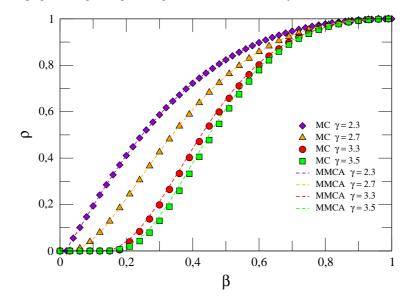
Fig. 3 Phase diagram for the SIS model ($\lambda = \infty$) in a random scale free network for different γ's. The networks size is $N = 10^4$ nodes and $\mu = 1$. MC results are averages over 10^2 realizations. Dashed lines corresponds to the theoretical prediction and symbols to MC results. After [26].

the SIS spreading process usually adopted [45], the classical result for uncorrelated SF networks is recovered because, in this case, the largest eigenvalue [16, 48] is $\Lambda_{\max} = \langle k^2 \rangle / \langle k \rangle$.

2.4 Mesoscopic equations at the critical point

Once the general framework given by the dynamical system (1, 2) has been proposed, it is instructive to approximate it using the hypotheses underlying HMF. These hypotheses consist of: i) coarse-graining the system in classes of node by degree, assuming that the dynamical properties within each class are the same, and ii) neglecting fluctuations. To obtain the mesoscopic description we consider the second order approximation of eqs. (4) and (5), and proceed as in the previous section. Therefore,

$$q_i \approx 1 - \beta \sum_j r_{ji}\varepsilon_j + \beta^2 \sum_{j<l} r_{ji}r_{li}\varepsilon_j\varepsilon_l . \qquad (10)$$

After substitution in (4) and reordering terms one gets

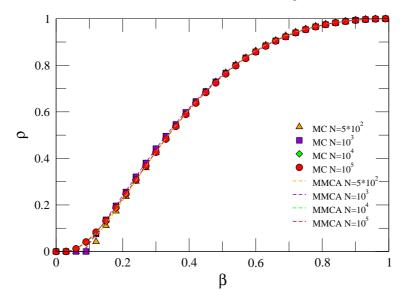$$0 = -\mu\varepsilon_i + \beta(1-\varepsilon_i)\sum_j r_{ji}\varepsilon_j + \mu\beta\varepsilon_i\sum_j r_{ji}\varepsilon_j - \beta^2 \sum_{j<l} r_{ji}r_{li}\varepsilon_j\varepsilon_l , \qquad (11)$$

Fig. 4 Phase diagram for the SIS model ($\lambda = \infty$) in a random scale free network for different system sizes as indicated. The networks have a power-law degree distribution with an exponent $\gamma = 2.7$ and $\mu = 1$. MC results are averages over 10^2 realizations. After [26].

which are the equations governing the dynamics of the contact-based epidemic spreading process at the microscopic level. It is possible to write eq. (11) at the commonly used mesoscopic (degree class) level for unweighted, undirected heterogeneous networks. The interactions then take place between classes of nodes. Defining the average density of infected nodes with degree k as $\rho_k = \frac{1}{N_k}\sum_{k_i=k} p_i$, where N_k is the number of nodes with degree k and the sum runs over the set of nodes of degree k, we obtain the generalized HMF equation near criticality.

To simplify the notation, we define the function

$$R_\lambda(x) = 1 - (1-x)^\lambda. \tag{12}$$

Thus, the values of r_{ji} may be expressed as

- Weighted networks:

$$r_{ji} = R_\lambda\left(\frac{w_{ji}}{w_j}\right). \tag{13}$$

- Unweighted networks:

$$r_{ji} = R_\lambda\left(\frac{a_{ji}}{k_j}\right) = a_{ji}R_\lambda\left(\frac{1}{k_j}\right) = a_{ji}R_\lambda(k_j^{-1}). \tag{14}$$

2.4.1 Homogeneous networks

For homogeneous unweighted undirected networks, $\varepsilon_i = \varepsilon$ and $k_i \approx \langle k \rangle$ for all nodes. Thus, $\rho = \frac{1}{N} \sum_j \varepsilon_j = \varepsilon$ and

$$0 = -\mu\rho + \beta\rho(1-\rho)\sum_j r_{ji} + \mu\beta\rho^2 \sum_j r_{ji} - \beta^2\rho^2 \sum_{j<l} r_{ji}r_{li}. \qquad (15)$$

The terms involving values of r_{ji} are

$$r_{ji} \approx a_{ji}R_\lambda(\langle k \rangle^{-1}), \qquad (16)$$

$$\sum_j r_{ji} \approx \langle k \rangle R_\lambda(\langle k \rangle^{-1}), \qquad (17)$$

$$\sum_{j<l} r_{ji}r_{li} \approx \frac{1}{2}\langle k \rangle(\langle k \rangle - 1)R_\lambda(\langle k \rangle^{-1})^2. \qquad (18)$$

Now, eq. (15) becomes

$$0 = -\mu\rho + \beta\rho(1-\rho)\langle k \rangle R_\lambda(\langle k \rangle^{-1})$$
$$+ \mu\beta\rho^2\langle k \rangle R_\lambda(\langle k \rangle^{-1}) - \beta^2\rho^2\frac{1}{2}\langle k \rangle(\langle k \rangle - 1)R_\lambda(\langle k \rangle^{-1})^2, \qquad (19)$$

which may be considered as the MF approximation of our model for homogeneous networks.

If $\lambda = 1$ then $R_1(\langle k \rangle^{-1}) = \frac{1}{\langle k \rangle}$ and eq. (19) becomes

$$0 = -\mu\rho + \beta\rho(1-\rho) + \mu\beta\rho^2 - \frac{\langle k \rangle - 1}{2\langle k \rangle}\beta^2\rho^2. \qquad (20)$$

If $\lambda \to \infty$ then $R_\infty(\langle k \rangle^{-1}) = 1$ and eq. (19) reads

$$0 = -\mu\rho + \beta\rho(1-\rho)\langle k \rangle + \mu\beta\rho^2\langle k \rangle - \frac{1}{2}\beta^2\rho^2\langle k \rangle(\langle k \rangle - 1). \qquad (21)$$

In both cases, the first two terms correspond to the standard CP and RP models (previously reported in the literature) respectively, and the additional terms are second order contributions corresponding to reinfections and multiple infections.

2.4.2 Heterogeneous networks

Now we will concentrate on the class of heterogeneous unweighted undirected networks completely specified by their degree distribution $P(k)$ and by the conditional probability $P(k'|k)$ that a node of degree k is connected to a node of degree k'. Of course, the normalization conditions $\sum_k P(k) = 1$ and $\sum_{k'} P(k'|k) = 1$ must be ful-

filled. In this case, the average number of links that goes from a node of degree k to nodes of degree k' is $kP(k'|k)$.

In these heterogeneous networks it is supposed that all nodes of the same degree behave equally, thus $\varepsilon_i = \varepsilon_j$ if $k_i = k_j$, and the density ρ_k of infected nodes of degree k is given by $\rho_k = \frac{1}{N_k}\sum_{i \in K}\varepsilon_i = \varepsilon_j$, $\forall j \in K$, where $N_k = P(k)N$ is the expected number of nodes with degree k. Here we have made use of K to denote the set of nodes with degree k. This notation allows to group the sums by the degrees of the nodes. For instance, if the degree of node i is $k_i = k$ then

$$\sum_j a_{ji}\varepsilon_j = \sum_{k'}\sum_{j \in K'} a_{ji}\rho_{k'} = \sum_{k'}\rho_{k'}\sum_{j \in K'} a_{ij} = \sum_{k'}\rho_{k'}kP(k'|k) = k\sum_{k'}P(k'|k)\rho_{k'}. \quad (22)$$

Now, let us find the mean field equation for heterogeneous networks. First we substitute equation 14 in equation 11

$$0 = -\mu\varepsilon_i + \beta(1-\varepsilon_i)\sum_j a_{ji}R_\lambda(k_j^{-1})\varepsilon_j$$
$$+ \mu\beta\varepsilon_i\sum_j a_{ji}R_\lambda(k_j^{-1})\varepsilon_j - \beta^2\sum_{j<l} a_{ji}a_{li}R_\lambda(k_j^{-1})R_\lambda(k_l^{-1})\varepsilon_j\varepsilon_l. \quad (23)$$

It is convenient to analize separately the summatory terms in equation 23, supposing node i has degree k:

$$\sum_j a_{ji}R_\lambda(k_j^{-1})\varepsilon_j = \sum_{k'}\sum_{j \in K'} a_{ji}R_\lambda(k'^{-1})\rho_{k'}$$
$$= \sum_{k'}R_\lambda(k'^{-1})\rho_{k'}\sum_{j \in K'} a_{ij}$$
$$= k\sum_{k'}P(k'|k)R_\lambda(k'^{-1})\rho_{k'}, \quad (24)$$

$$\sum_{j<l} a_{ji}a_{li}R_\lambda(k_j^{-1})R_\lambda(k_l^{-1})\varepsilon_j\varepsilon_l$$
$$= \frac{1}{2}\sum_j\sum_l a_{ji}a_{li}R_\lambda(k_j^{-1})R_\lambda(k_l^{-1})\varepsilon_j\varepsilon_l - \frac{1}{2}\sum_j a_{ji}^2 R_\lambda(k_j^{-1})^2\varepsilon_j^2$$
$$= \frac{1}{2}\sum_{k'}\sum_{k''}\sum_{j \in K'}\sum_{l \in K''} a_{ji}a_{li}R_\lambda(k'^{-1})R_\lambda(k''^{-1})\rho_{k'}\rho_{k''} - \frac{1}{2}\sum_{k'}\sum_{j \in K'} a_{ji}^2 R_\lambda(k'^{-1})^2\rho_{k'}^2$$
$$= \frac{1}{2}\sum_{k'}\sum_{k''}R_\lambda(k'^{-1})R_\lambda(k''^{-1})\rho_{k'}\rho_{k''}\sum_{j \in K'} a_{ij}\sum_{l \in K''} a_{il} - \frac{1}{2}\sum_{k'}R_\lambda(k'^{-1})^2\rho_{k'}^2\sum_{j \in K'} a_{ij}^2$$
$$= \frac{1}{2}k^2\sum_{k'}\sum_{k''}R_\lambda(k'^{-1})R_\lambda(k''^{-1})P(k'|k)P(k''|k)\rho_{k'}\rho_{k''}$$
$$- \frac{1}{2}k\sum_{k'}R_\lambda(k'^{-1})^2 P(k'|k)\rho_{k'}^2. \quad (25)$$

Substitution in equation 23 leads to the generalized HMF equation

$$
\begin{aligned}
0 = &-\mu\rho_k + \beta k(1-\rho_k)\sum_{k'}P(k'|k)R_\lambda(k'^{-1})\rho_{k'} \\
&+ \mu\beta k\rho_k\sum_{k'}P(k'|k)R_\lambda(k'^{-1})\rho_{k'} \\
&- \frac{1}{2}\beta^2 k^2\sum_{k'}\sum_{k''}R_\lambda(k'^{-1})R_\lambda(k''^{-1})P(k'|k)P(k''|k)\rho_{k'}\rho_{k''} \\
&+ \frac{1}{2}\beta^2 k\sum_{k'}R_\lambda(k'^{-1})^2 P(k'|k)\rho_{k'}^2\,.
\end{aligned}
\tag{26}
$$

If $\lambda = 1$ then $R_1(k^{-1}) = \frac{1}{k}$ and eq. (26) becomes

$$
\begin{aligned}
0 = &-\mu\rho_k + \beta k(1-\rho_k)\sum_{k'}\frac{1}{k'}P(k'|k)\rho_{k'} \\
&+ \mu\beta k\rho_k\sum_{k'}\frac{1}{k'}P(k'|k)\rho_{k'} + \frac{1}{2}\beta^2 k\sum_{k'}\frac{1}{k'^2}P(k'|k)\rho_{k'}^2 \\
&- \frac{1}{2}\beta^2 k^2\left(\sum_{k'}\frac{1}{k'}P(k'|k)\rho_{k'}\right)^2\,.
\end{aligned}
\tag{27}
$$

If $\lambda \to \infty$ then $R_\infty(k^{-1}) = 1$ and eq. (26) reads

$$
\begin{aligned}
0 = &-\mu\rho_k + \beta k(1-\rho_k)\sum_{k'}P(k'|k)\rho_{k'} \\
&+ \mu\beta k\rho_k\sum_{k'}P(k'|k)\rho_{k'} + \frac{1}{2}\beta^2 k\sum_{k'}P(k'|k)\rho_{k'}^2 \\
&- \frac{1}{2}\beta^2 k^2\left(\sum_{k'}P(k'|k)\rho_{k'}\right)^2\,.
\end{aligned}
\tag{28}
$$

Again, the first two terms in both cases correspond to the standard CP and RP HMF equations respectively, and the additional terms are second order contributions corresponding to reinfections and multiple infections.

3 Traffic-driven epidemic spreading in complex networks

In the second part of this chapter we investigate the outcome of an epidemic spreading process driven by transport instead of diffusion. To this end, we analyzed a paradigmatic abstraction of epidemic contagion, the so-called Susceptible-Infected-Susceptible (SIS) model, which assumes that contagion occurs through the eventual contact or transmission between connected partners that are using their connections

at the time of propagation. This is achieved by considering a quantized interaction at each time step. Mathematically, we set up the model in a flow scenario where contagion is carried by interaction packets traveling across the network.

3.1 The model

In the first place, two different types of SF networks are generated. On one hand, we build random uncorrelated SF networks using the configuration model [6, 21]. On the other hand, small-world, SF and highly clustered networks – all properties found in many real-world networks [6, 21] such as the Internet – are also generated using a class of recently developed network models [50, 9], in which nearby nodes in a hidden metric space are connected. This metric space can represent social, geographical or any other relevant distance between the nodes of the simulated networks. Specifically, in the model currently at study, nodes are uniformly distributed in a one-dimensional circle by assigning them a random polar angle θ distributed uniformly in the interval $[0, 2\pi)$ and assigned an expected degree k. The expected degrees of the nodes are then drawn from some distribution $x(k)$ and the network is completed by connecting two nodes with hidden coordinates (θ, k) and (θ', k') with probability $r(\theta, k, \theta', k') = \left(1 + \frac{d(\theta, \theta')}{\eta' k k'}\right)^{-\alpha}$, where $\eta' = (\alpha - 1)/2\langle k \rangle$, $d(\theta, \theta')$ is the geodesic distance between the two nodes on the circle, and $\langle k \rangle$ is the average degree. Finally, choosing $x(k) = (\gamma - 1)k_0^{\gamma-1}k^{-\gamma}$, $k > k_0 \equiv (\gamma - 2)\langle k \rangle/(\gamma - 1)$ generates random networks with a power law distribution with exponent $\gamma > 2$. In most of the simulations, $\gamma = 2.7$ $\langle k \rangle = 3$ and $\alpha = 2$ are fixed.

Once the networks are built up, the traffic process is implemented in the following way. At each time step, $p = \Lambda N$ new packets are created with randomly chosen origins and destinations. For the sake of simplicity, packets are considered non-interacting so that no queues are used. The routing of information is modeled through even a shortest path delivery strategy or a greedy algorithm [9, 8]. In the latter, the second class of SF networks is used and a node i forwards a packet to node j in its neighborhood, which is the closest node (in the hidden metric space) to the final packet destination. Results are insensitive to the two routing protocols implemented.

To model the spreading dynamics we have implemented the aforementioned Susceptible-Infected-Susceptible model, in which each node can be in two possible states: healthy (S) or infected (I). Starting from an initial fraction of infected individuals $\rho_0 = I_0/N$, the infection spreads in the system as the nodes interact. A susceptible node has a probability β of becoming infected every time it interact with an infected neighbors. We also assume that infected nodes are recovered at a rate μ, which we fix to 1 for most of the simulations. After a transient time, we compute the average density of infected individuals, ρ, which is the prevalence of disease in the system. To account for link concurrency, we consider that two nodes do not interact at all times t, but only when they exchange at least a packet. This

situation is reminiscent of disease transmission on air transportation networks; if an infected individual did not travel between two cities, then regardless of whether or not those cities are connected by a direct flight, the epidemic will not spread from one place to the other. In this way, although a node can potentially interact with as many contacts as it has and as many times as packets it exchanges with its neighbors, the effective interactions are driven by a second dynamics (traffic). The more packets travel through a link, the more likely the disease will spread through it. On the other hand, once an interaction is at work, the epidemics spreads from infected to susceptible nodes with probability β. For example, if at time t node i is infected and a packet is travelling from node i to one of its neighbors node j, then at the next time step, node j will be infected with probability β. Therefore, susceptible and infected states are associated with the nodes, whereas the transport of packets is the mechanism responsible for the propagation of the disease at each time step.

3.2 Unbounded delivery rate

We firstly concentrate on an unbounded delivery rate scenario, in which every node can handle as much packets it receives. In this situation, congestion can not arise in the system. Fig. 5 shows the results for the stationary density of infected nodes ρ as a function of β and the traffic generation rate Λ for SF networks.

In this case the traffic level determines the value of both the epidemic incidence and the critical thresholds and it's important to notice the emergence of an epidemic threshold under low traffic conditions. This implies that for a fixed value of Λ, the epidemic dies out if the spreading rate is below a certain critical value $\beta_c(\Lambda)$. More intense packet flows yield lower epidemic thresholds. The reason for the dependence of the critical spreading rates on Λ is rooted in the effective topological paths induced by the flow of packets through the network. At low values of Λ, there are only a few packets traveling throughout the system, so the epidemic simply dies out because many nodes do not participate in the interaction via packets exchanges. As Λ grows, more paths appear between communicating nodes, thus spreading the infection to a larger portion of the network. Therefore, in traffic-driven epidemic processes the infection is constrained to propagate only through links that transmit a packet, and thus the number of attempts to transmit the infection depends on the flow conditions at a local level, namely, on the number of active communication channels at each time step. As a consequence, the effective network that spreads the infection is no longer equivalent to the complete underlying topology. Instead, it is a map of the dynamical process associated with packet traffic flow. The conclusion is that the disease propagation process has two dynamical components: one intrinsic to the disease itself (β) and the other to the underlying traffic dynamics (the flow). To theorize about these effects we next formulate the analytical expression for the dependence of the epidemic threshold on the amount of traffic injected into the system, following a mean-field approach akin to the conventional analysis of the reaction driven case. Mathematically, the fraction of paths traversing a node given
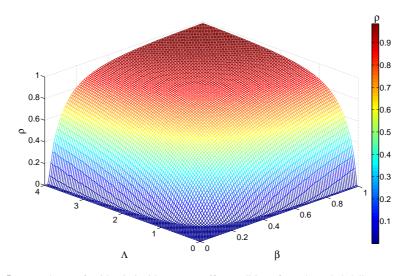
Fig. 5 Dependence of epidemic incidence on traffic conditions for unbounded delivery rate. The density of infected nodes, ρ, is shown as a function of the spreading rate β and the intensity of flow Λ in SF networks. Flow conditions (controlled by Λ) determine both the prevalence level and the values of the epidemic thresholds. Increasing the number of packets traveling through the system has a malicious effect: the epidemic threshold decreases as the flow increases. Each curve is an average of 10^2 simulations starting from an initial density of infected nodes $\rho_0 = 0.05$. The network is made up of 10^3 nodes using the model in [9], results correspond to the greedy routing scheme. The remaining parameters are $\alpha = 2$, $\gamma = 2.6$ and $\langle k \rangle = 3$. After [37].

a certain routing protocol [27], the so-called algorithmic betweenness, b_{alg}^k, defines the flow pathways. Let us consider the evolution of the relative density, $\rho_k(t)$, of infected nodes with degree k. Following the heterogeneous mean-field approximation [45], the dynamical rate equations for the SIS model are

$$\partial_t \rho_k(t) = -\mu \rho_k(t) + \beta \Lambda b_{alg}^k N [1 - \rho_k(t)] \Theta(t). \qquad (29)$$

The first term in Eq. (29) is the recovery rate of infected individuals (we set henceforth $\mu = 1$). The second term takes into account the probability that a node with k links belongs to the susceptible class, $[1 - \rho_k(t)]$, and gets the infection via packets traveling from infected nodes. The latter process is proportional to the spreading probability β, the probability $\Theta(t)$ that a packet travels through a link pointing to an infected node and the number of *packets* received by a node of degree k. This, in turns, is proportional to the total number of packets in the system, $\sim \Lambda N$, and the algorithmic betweenness of the node, b_{alg}^k. Note that the difference with the standard epidemic spreading model is given by these factors, as now the number of contacts per unit time of a node is not proportional to its connectivity but to the number of packets that travel through it. Finally, $\Theta(t)$ takes the form

$$\Theta(t) = \frac{\sum_k b_{alg}^k P(k)\rho_k(t)}{\sum_k b_{alg}^k P(k)}. \tag{30}$$

Eq. (29) has been obtained assuming: (i) that the network is uncorrelated $P(k'|k) = k'P(k')/\langle k\rangle$, and (ii) that the algorithmic flow between the classes of nodes of degree k and k' factorizes $b_{alg}^{kk'} \sim b_{alg}^k b_{alg}^{k'}$. Although no uncorrelated networks exist, this approximation allows us to identify the governing parameters of the proposed dynamics. The second approximation is an upper bound to the actual value of the $b_{alg}^{kk'}$, whose mathematical expression is, in general, unknown. The validity of the theory even with these approximations is notable as confirmed by the numerical simulations.

By imposing stationarity $[\partial_t \rho_k(t) = 0]$, Eq. (29) yields

$$\rho_k = \frac{\beta \Lambda b_{alg}^k N\Theta}{1 + \beta \Lambda b_{alg}^k N\Theta}, \tag{31}$$

from which a self-consistent equation for Θ is obtained as

$$\Theta = \frac{1}{\sum_k b_{alg}^k P(k)} \sum_k \frac{(b_{alg}^k)^2 P(k)\beta \Lambda N\Theta}{1 + \beta \Lambda b_{alg}^k N\Theta}. \tag{32}$$

The value $\Theta = 0$ is always a solution. In order to have a non-zero solution, the condition

$$\frac{1}{\sum_k b_{alg}^k P(k)} \frac{d}{d\Theta} \left(\sum_k \frac{(b_{alg}^k)^2 P(k)\beta \Lambda N\Theta}{1 + \beta \Lambda b_{alg}^k N\Theta} \right)\Bigg|_{\Theta=0} > 1 \tag{33}$$
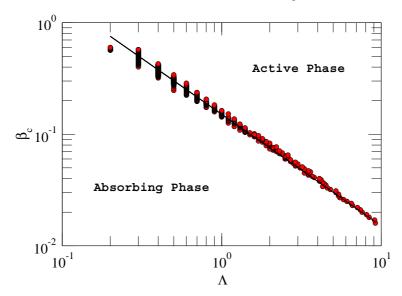
must be fulfilled, from which the epidemic threshold is obtained as

$$\beta_c = \frac{\langle b_{alg}\rangle}{\langle b_{alg}^2\rangle} \frac{1}{\Lambda N}, \tag{34}$$

below which the epidemic dies out, and above which there is an endemic state. In Fig. 6 a comparison between the theoretical prediction and numerical observations is presented. Here, we have explicitly calculated the algorithmic betweenness for the greedy routing as it only coincides with the topological betweenness for shortest paths routing. The obtained curve separates two regions: an absorbing phase in which the epidemic disappears, and an active phase where the infection is endemic.

Equation (34) is notably simple but has profound implications: the epidemic threshold decreases with traffic and eventually vanishes in the limit of very large traffic flow in finite systems, in contrast to the expected result of a finite-size reminiscent threshold in the classical reactive–diffusive framework. Admittedly, this is a new feature with respect to previous results on epidemic spreading in SF networks. It is rooted in the increase of the effective epidemic spreading rate due to the flow of packets. This is a genuine effect of traffic-driven epidemic processes and generalizes

Fig. 6 Comparison between numerical and theoretical critical points. Log-log plot of the critical thresholds, β_c, as a function of the rate at which packets are injected into the system, Λ. Two regions are differentiated: an active and an absorbing phase as indicated. The solid line corresponds to Eq. (34) with $\frac{\langle b_{alg} \rangle}{\langle b_{alg}^2 \rangle} \frac{1}{N} = 0.154$. The agreement is remarkable even though Eq. (34) is derived using a MF approach. The underlying network, infection spreading mechanism and routing protocol are the same as in Fig. 5. Each curve is an average of 10^2 simulations. Remaining parameters are the same as in Fig. 5. After [37].

the hypothesis put forward in the framework of a reaction-diffusion process [18] on SF networks. It implies that an epidemic will pervade the (finite) network whatever the spreading rate is if the load on it is high enough. Moreover, Eq. (34) reveals a new dependence. The critical threshold depends on the topological features of the graph, but at variance with the standard case, through the first two moments of the algorithmic betweenness distribution. As noted above, the algorithmic betweenness of a node is given by the number of packets traversing that node given a routing protocol. In other words, it has two components: a topological one which is given by the degree of the node and a dynamical component defined by the routing protocol.

Within our formulation, the classical result [45]

$$\beta_c = \frac{\langle k \rangle}{\langle k^2 \rangle}, \tag{35}$$

can be obtained for a particular protocol and traffic conditions, although we note that the microscopic dynamics of our model is different from the classical SIS. To see this, assume a random protocol. If packets of information are represented as w random walkers traveling in a network with average degree $\langle k \rangle$, then under the assumption that the packets are not interacting, it follows that the average number
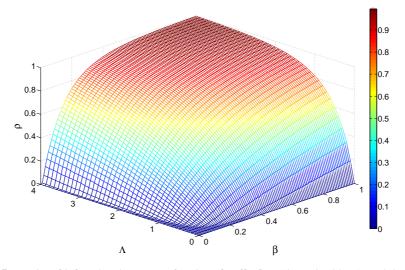
Fig. 7 Density of infected nodes, ρ, as a function of traffic flow (determined by Λ) and the epidemic spreading rate β for random scale-free networks and a shortest paths routing scheme for packets delivery. Each point is the result of 10^2 averages over different networks and initial conditions. The exponent of the degree distribution of the network is $\gamma = 2.7$. After [37].

of walkers at a node i in the stationary regime (the algorithmic betweenness) is given by [44, 36] $b^i_{alg} = \frac{k_i}{N\langle k \rangle} w$. The effective critical value is then $(\beta\Lambda)_c = \langle k \rangle^2 / (\langle k^2 \rangle w)$, that recovers, when $\omega = \langle k \rangle$, the result in Eq. (35).

Results are robust for other network models and different routing algorithms. We have also made numerical simulations of the traffic-driven epidemic process on top of Barabási-Albert and random SF networks implementing a shortest paths delivery scheme. In this case, packets are diverted following the shortest path (in the actual topological space) from the packets' origins to their destinations. The rest of model parameters and rules for epidemic spreading remain the same. Figs. 7 and 8 show the results obtained for random SF networks generated via the configuration model and the Barabási-Albert model respectively. As can be seen, the phenomenology is the same for both types of networks: the epidemic threshold depends on the amount of traffic in the network such that the higher the flow is, the smaller the epidemic threshold separating the absorbing and active phases. On the other hand, for processes in which the delivery of packets follows a shortest path algorithm, Eq. (34) looks like

$$\beta_c = \frac{\langle b_{top} \rangle}{\langle b_{top}^2 \rangle} \frac{1}{\Lambda N}, \qquad (36)$$

where b_{top} is the topological betweenness. To further confirm our findings on a realistic topology we run the model on top of the Air Transportation Network (ATN) [28]. The network composed by the direct flies between more the 3000 airports in the world, in which each node represents an airport and the links represents the direct connection between them. Although in the ATN links have weights accounting for
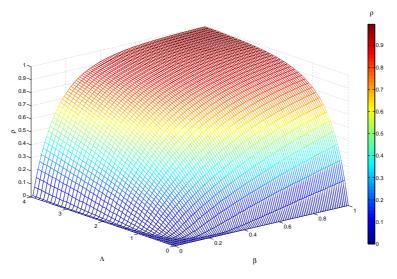
Fig. 8 Density of infected nodes, ρ, as a function of traffic flow (determined by Λ) and the epidemic spreading rate β for BA scale-free networks and a shortest paths routing scheme for packets delivery. Each point is the result of 10^2 averages over different networks and initial conditions. After [37].

the annual number of passengers voyaging on each connection, we considered the network as un-weighted and the shortest-path routing protocol. Also in this case the results are confirmed as shown in Fig. 9. Fig. 10 also shows the agreement between the analytical prediction and the numerical simulations.

3.3 Bounded delivery rate

Equation (36) allows us to investigate also the equivalent scenario in the presence of congestion. Let us consider the same traffic process above but with nodes having queues that can store as many packets as needed but can deliver, on average, only a finite number of them at each time step. It is known that there is a critical value of Λ above which the system starts to congest [27]

$$\Lambda_c = \frac{(N-1)}{b_{alg}^*}. \tag{37}$$

Equation (37) gives the traffic threshold that defines the onset of congestion, which is governed by the node with maximum algorithmic betweenness b_{alg}^*. Substituting (37) in (34) we obtain a critical threshold for an epidemic spreading process bounded by congestion. Increasing the traffic above Λ_c will gradually congest all
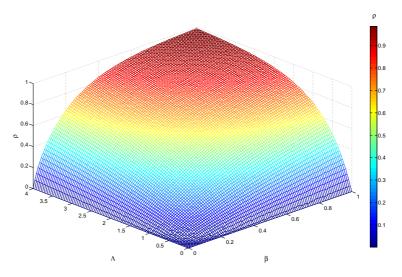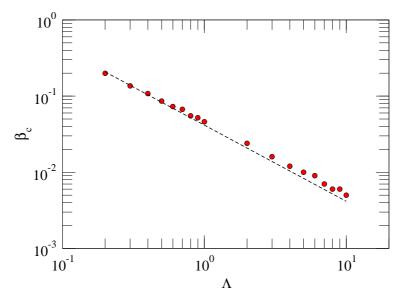
Fig. 9 Density of infected nodes, ρ, as a function of traffic flow (determined by Λ) and the epidemic spreading rate β for the ATN (considered as unweighted) and a shortest paths routing scheme for packets delivery. Each point is the result of 10^2 averages over different networks and initial conditions. After [37].

the nodes in the network up to a limit in which the traffic is stationary and the lengths of queues grow without limit.

To illustrate this point, let us assume that the capacities for processing and delivering information are heterogeneously distributed [54, 52, 49] so that the larger the number of paths traversing a node, the larger its capability to deliver the packets. Specifically, each node i of the network delivers at each time step a maximum of $\lceil c_i = 1 + k_i^\eta \rceil$ packets, where η is a parameter of the model. In this case, the critical value of Λ in Eq.(37) is multiplied by the maximum delivery capacity [54]. Moreover, without loss of generality, we will explore the behavior of the model in random SF networks where the routing is implemented by shortest paths $b_{alg} = b_{top} \sim k^\nu$, being ν usually between 1.1 and 1.3 [47]. The previous assumption for the delivery capability thus allows to explore as a function of η the situations in which the delivery rate is smaller or larger than the arrival rate (defined by the algorithmic betweenness). Phenomenologically, these two scenarios correspond to the cases in which the traffic is in a free flow regime (if $\eta > \nu$) or when the network will congest (if $\eta < \nu$). We also note that the adopted approach is equivalent to assume a finite length for the queues at the nodes.

Fig. 11 shows the fraction of active packets on the network, as a function of the spreading rate β and the rate at which packets are generated Λ for two different values of η using a shortest path delivery scheme on top of random SF networks. For $\eta = 0.8$, the epidemic incidence is significantly small for all values of the parameters Λ and β as compared with the results obtained when the rate of packets delivery is unbounded. On the contrary, when $\eta = 1.7$ the phase diagram is qualitatively the

Fig. 10 Comparison between numerical and theoretical critical points in the ATN. Log-log plot of the critical thresholds, β_c, as a function of the rate at which packets are injected into the system, Λ for the ATN. The dashed line corresponds to Eq. (34) with $\frac{\langle b_{alg} \rangle}{\langle b_{alg}^2 \rangle} \frac{1}{N} = 0.041$. Despite existing degree correlations in the network, the agreement is remarkable. Each point is an average of 10^2 simulations. After [37].

same as for the unbounded case, including the result that the epidemic incidence vanishes when Λ is large enough. A closer look at the dynamical evolution unveils an interesting, previously unreported, feature − when the rate at which packets are delivered is smaller than the rate at which they arrive, the average value of infected nodes saturates beyond a certain value of the traffic flow rate Λ. This effect is due to the emergence of traffic congestion. When the flow of packets into the system is such that nodes are not able to deliver at least as many packets as they receive, their queues start growing and packets pile up. This in turns implies that the spreading of the disease becomes less efficient, or in other words, the spreading process slows down. The consequence is that no matter whether more packets are injected into the system, the average level of packets able to move from nodes to nodes throughout the network is roughly constant and so is the average level of infected individuals.

Fig. 12 illustrates the phenomenological picture described above. It shows the epidemic incidence ρ for a fixed value of $\beta = 0.15$ as a function of Λ for different values of η. The figure clearly evidences that congestion is the ultimate reason of the behavior described above. Therefore, the conclusion is that in systems where a traffic process with finite delivery capacity is coupled to the spreading of the disease the *epidemic incidence is bounded*. This is good news as most of the spreading processes in real-world networks involves different traffic flow conditions. Further evidence of this phenomenology is given in Fig. 13, where we have depicted the
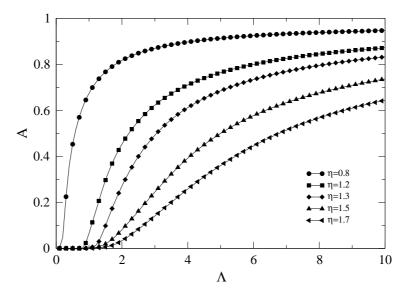
Fig. 11 Fraction of active packets as a function of the traffic flow with bounded delivery rate. It represents the fraction of active packets A: packets still traveling in the network over the total amount of generated packets in a time period τ, as function of the traffic injected in the system Λ for different values of the delivery capacity η. The underlying network and the routing protocol are the same as in Fig. 7. After [37].

epidemic threshold as a function of Λ for two different values of η, less and greater than ν. When $\eta < \nu$ congestion arises, and the contrary holds for $\eta > \nu$ where the diagram is equivalent to that of unbounded traffic. The onset of congestion determines the value of β above which congestion starts. It is clearly visualized as the point beyond which the power law dependence in Eq. (34) breaks down. The plateau of β_c corresponds to the stationary situation of global congestion. A comparison for different values of η in the bounded delivery rate model is presented in Fig. 14.

4 Conclusions

In the first part of this chapter we have presented a novel framework, the Microscopic Markov-Chain Approach, to study disease spreading in networks. By defining a set of discrete-time equations for the probability of individual nodes to be infected, we construct a dynamical system that generalizes from an individual contact process to the classical case in which all connections are concurrently used, for any complex topology. The whole phase diagram of the system can be found solving the equations at the stationary state. The numerical solution of the analytic equations overcomes the computational cost of MC simulations. Moreover, the formalism allows to gain insight on the behavior of the critical epidemic threshold for
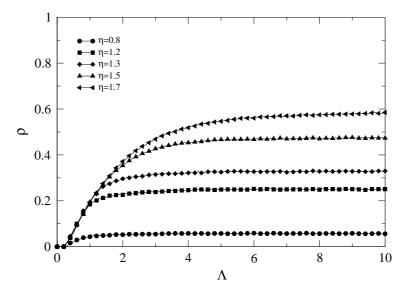
Fig. 12 Epidemic incidence in traffic-driven epidemic processes with bounded delivery rate. The figure represents the average fraction of infected nodes ρ as a function of Λ for different delivery rates at fixed $\beta = 0.15$. When congestion arises, the curves depart from each other and the epidemic incidence saturates soon afterwards. After [37].

different values of the probability of contacting a fraction λ of neighbors per time step.

The MMCA model deals with infections driven by direct contacts between nodes, but not with traffic situations where nodes transmit the epidemics by flow communication with others [37]. In this latter case, the routing protocol of traffic between nodes is absolutely relevant and can change the critical point of the epidemic spreading.

In the second part of this chapter we have developed a framework in the scope of MF theories to cope with the problem of assessing the impact of epidemics when the routing of traffic is considered. We have argued both analytically and numerically the conditions for the emergence of an epidemic outbreak in scale-free networks when disease contagion is driven by traffic or interaction flow. The study provides a more general theory of spreading processes in complex heterogeneous networks that includes the previous results as a particular case of diffusive spreading. Moreover, we have shown that the situation in which the epidemic threshold vanishes in finite scale-free networks is also plausible, thus providing an explanation to the long-standing question of why some viruses prevail in the system with a low incidence.

The new approach presented here provides a novel framework to address related problems. For instance, in the context of air-transportation networks [17], a similar mechanism to the one reported here could explain the observed differences in the impact of a disease during a year [25]. One might even expect that, due to seasonal fluctuations in flows, the same disease could not provoke a system-wide outbreak
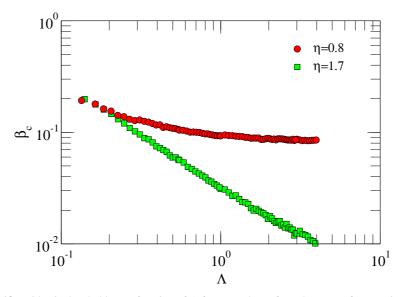
Fig. 13 Epidemic thresholds as a function of Λ for two values of η. The onset of congestion (the arrow in the plot) marks the point, $\Lambda_c \approx 0.150$, at which the curve for $\eta = 0.8$ departs from Eq. (34), i.e., when the power law dependence breaks down. Soon afterwards congestion extends to the whole network leading to a bounded (from below) epidemic threshold. On the contrary, when the delivery rate is large enough (as in the case of $\eta = 1.7$), Eq. (34) holds for all values of Λ, thus resembling the unbounded delivery rate case. After [37].

if the flow were not high enough during the initial states of the disease contagion. Incorporating the non-diffusive character of the spreading process into current models has profound consequences for the way the system functions. Also the theory could help designing new immunization algorithms or robust protocols; one in particular being quarantining highly sensitive traffic nodes. On more general grounds, our conclusions point to the need of properly dealing with link concurrency. Further exploring this challenge will have far-reaching consequences for the study of dynamical processes on networks, and especially the relationship between structure and dynamics for networked systems. Ultimately, this paves the way towards a more complete theoretical framework of complex networks.
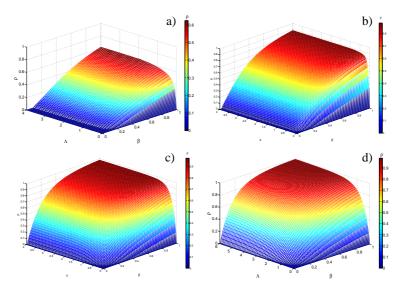
Fig. 14 Comparison between different delivery capacity in the bounded delivery rate model. The plot represents density of infected nodes, ρ, as a function of traffic flow Λ and the epidemic spreading rate β for random scale-free networks and a shortest paths routing scheme with different values of the delivery capacity η: panel a) $\eta = 0.8$, b) $\eta = 1.0$, c) $\eta = 1.5$ and d) $\eta = 1.7$, for the random SF network and the shortest path delivery scheme. After [37].

References

1. Amaral, L. A. N. , Scala, A., Barthélemy, M., Stanley, H. E. Classes of small-world networks. *Proc. Nat. Acad. Sci. USA* 97:11149-11152. (2000)
2. Anderson, R. M., May, R. M. *Infectious diseases of humans: Dynamics and Control*. (Oxford University Press, Oxford). (1992)
3. Barabási, A. L., Albert, R. Emergence of scaling in random networks. *Science* 286:509-512. (1999)
4. Barthélemy, M., Barrat, A., Pastor-Satorras, R., Vespignani A. Velocity and hierarchical spread of epidemic outbreaks in scale-free networks. *Phys. Rev. Lett.* 92:178701. (2004)
5. Barrat, A., Barthélemy, M., Pastor-Satorras, R., Vespignani, A. The architecture of complex weighted networks. *Proc. Natl. Acad. Sci. USA* 101:3747-3752. (2004)
6. Boccaletti, S., Latora, V., Moreno, Y., Chávez, M., Hwang, D. U. Complex Networks: Structure and Dynamics. *Phys. Rep.* 424:175-308. (2006)
7. Boguña, M., Castellano, C., Pastor-Satorras, R. Langevin approach for the dynamics of the contact process on annealed scale-free networks. *Phys. Rev. E* 79:036110. (2009)
8. Boguñá, M., Krioukov, D. Navigating Ultrasmall Worlds in Ultrashort Time. *Phys. Rev. Lett.* 102:058701. (2009)
9. Boguñá, M., Krioukov, D., Claffy, K. C. Navigability of Complex Networks. *Nature Physics* 5:74-80. (2009)
10. Caldarelli, G. *Scale-Free Networks*. (Oxford University Press, Oxford). (2007)
11. Castellano, C., Pastor-Satorras, R. Non-mean-field behavior of the contact process on scale-free networks. *Phys. Rev. Lett.* 96:038701. (2006)
12. Castellano, C., Pastor-Satorras, R. Reply: Non-mean-field behavior of the contact process on scale-free networks. *Phys. Rev. Lett.* 98:029802. (2007)

13. Castellano, C., Pastor-Satorras, R. Routes to thermodynamic limit on scale-free networks. *Phys. Rev. Lett.* 100:148701. (2008)
14. Catanzaro, M., Boguña, M., Pastor-Satorras, R. Diffusion-annihilation processes in complex networks. *Phys. Rev. E* 71:056104. (2005)
15. Chakrabarti, D., Wang, Y., Wang, C., Leskovec, J., Faloutsos, C. Epidemic thresholds in real networks. *ACM Trans. Inf. Syst. Secur.* 10(4):13. (2008)
16. Chung, F., Lu, L., Vu, V. Spectra of random graphs with given expected degrees. *Proc. Natl. Acad. Sci. USA* 100:6313-6318. (2003)
17. Colizza, V., Barrat, A., Barthélemy, M., Vespignani, A. Predictability and epidemic pathways in global outbreaks of infectious diseases: the SARS case study. *BMC Medicine* 5:34. (2007)
18. Colizza, V., Pastor-Satorras, R., Vespignani A. Reaction-diffusion processes and metapopulation models in heterogeneous networks. *Nature Physics* 3:276-282. (2007)
19. Colizza, V., Vespignani, A. Epidemic modeling in metapopulation systems with heterogeneous coupling pattern: Theory and simulations. *Journal of Theoretical Biology* 251:450-467. (2008)
20. Daley, D. J., Gani, J. *Epidemic Modelling*. (Cambridge University Press, Cambridge). (1999)
21. Dorogovtsev, S. N, Goltsev, A. V., Mendes, J. F. F. Critical phenomena in complex networks. *Rev. Mod. Phys.* 80:1275-1336. (2008)
22. Eubank, S., Guclu, H., Anil-Kumar, V. S., Marathe, M. V., Srinivasan, A., Toroczkai, Z., Wang N. Modelling disease outbreaks in realistic urban social networks. *Nature* 429:180-184. (2004)
23. Gallos, L. K., Argyrakis, P. Absence of Kinetic Effects in Reaction-diffusion processes in scale-free Networks. *Phys. Rev. Lett.* 92:138301. (2004)
24. Gardeñes, J.G., Latora, V., Moreno, Y., Profumo, E. Spreading of sexually transmitted diseases in heterosexual populations. *Proc. Nat. Acad. Sci. USA* 105:1399-1404. (2008)
25. Grais, R. F., Ellis, J. H., Kress, A., Glass, G. E. Modeling the spread of annual influenza epidemics in the U.S.: The potential role of air travel. *Health Care Management Science* 7:127-134. (2004)
26. Gómez, S., Arenas, A., Borge-Holthoefer, J., Meloni, S., Moreno, Y. Discrete-time Markov chain approach to contact-based disease spreading in complex networks. *Europhys. Lett.* 89:38009. (2010)
27. Guimerà, R., Díaz-Guilera, A., Vega-Redondo, F., Cabrales, A., Arenas, A. Optimal network topologies for local search with congestion. *Phys. Rev. Lett.* 89:248701. (2002)
28. Guimerà, R., Mossa, S., Turtschi, A., Amaral, L. A. N. The worldwide air transportation network: Anomalous centrality, community structure, and cities' global roles. *Proc. Natl. Acad. Sci. USA* 102:7794-7799. (2005)
29. Ha, M., Hong, H., Park, H. Comment: Non-mean-field behavior of the contact process on scale-free networks. *Phys. Rev. Lett.* 98:029801. (2007)
30. Han, J.-D. J., Bertin, N., Hao, T., Goldberg, D. S. et al Evidence for dynamically organized modularity in the yeast protein-protein interaction network. *Nature* 430: 88-93. (2004)
31. Hethcote, H. W. The mathematics of infectious diseases. *SIAM Review* 42:599-653. (2000)
32. Hufnagel, L., Brockmann, D., Geisel T. Forecast and control of epidemics in a globalized world. *Proc. Natl. Acad. Sci. USA* 101:1512415129. (2004)
33. Liljeros F., Edling C. R., Amaral L. A. N., Stanley H. E., Aberg Y. The Web of Human Sexual Contacts. *Nature* 411:907-908. (2001)
34. LLoyd, A. L., May, R. M. How viruses spread among computers and people. *Science* 292:1316-1317. (2001)
35. Marro, J., Dickman, R. *Nonequilibrium phase transitions in lattice models*. (Cambridge University Press, Cambridge). (1999)
36. Meloni, S., Gardeñes, J.G., Latora, V., Moreno, Y. Scaling Breakdown in Flow Fluctuations on Complex Networks. *Phys. Rev. Lett.* 100:208701. (2008)
37. Meloni, S., Arenas, A., Moreno Y. Traffic-Driven Epidemic Spreading in Finite-Size Scale-Free Networks. *Proc. Natl. Acad. Sci. USA* 106:16897-16902. (2009)
38. Moreno, Y., Pastor-Satorras, R. Vespignani, A. Epidemic outbreaks in complex heterogeneous networks. *Eur. Phys. J. B* 26:521-529. (2002)

39. Murray J. D. *Mathematical Biology*. (Springer-Verlag, Germany, Berlin). (2002)
40. Murray, J. D. *Mathematical Biology*. (Springer-Verlag, 3rd Edition). (2007)
41. Newman, M. E. J. The spread of epidemic disease on networks. *Phys. Rev. E* 66:016128. (2002)
42. Newman, M. E. J. The structure and function of complex networks. *SIAM Review* 45:167-256. (2003)
43. Newman, M. E. J., Forrest, S., Balthrop, J. Email networks and the spread of computer viruses. *Phys. Rev. E* 66:035101. (2002)
44. Noh, J. D., Rieger, H. Random Walks on Complex Networks. *Phys. Rev. Lett.* 92:118701. (2004)
45. Pastor-Satorras, R., Vespignani, A. Epidemic spreading in scale-free networks. *Phys. Rev. Lett.* 86:3200-3203. (2001)
46. Pastor-Satorras, R., Vespignani A. Epidemic dynamics and endemic states in complex networks. *Phys. Rev. E* 63:066117. (2001)
47. Pastor-Satorras, R., Vespignani A. *Evolution and Structure of the Internet: a statistical physics approach*. (Cambridge University Press, Cambridge). (2004)
48. Restrepo, J. G., Ott, E., Hunt, B. R. Approximating the largest eigenvalue of network adjacency matrices. *Phys. Rev. E* 76:056119. (2007)
49. Rosato, V., Meloni, S., Issacharoff, L., Tiriticco, F. Is the topology of the internet network really fit to its function? *Physica A* 387:1689-1704. (2008)
50. Serrano, M. A. , Krioukov, D., Boguñá, M. Self-Similarity of Complex Networks and Hidden Metric Spaces. *Phys. Rev. Lett.* 100:078701. (2008)
51. Shao, J., Buldyrev, S. V., Braunstein, L. A., Havlin, S., Stanley, E. Structure of shells in complex networks. *Phys. Rev. E* 80:036105. (2009)
52. Sreenivasan, S., Cohen, R., Lopez, E., Toroczkai, Z., Stanley, H. E. Structural Bottlenecks for Communication in Networks. *Phys. Rev. E* 75:036105. (2007)
53. Stanley, H. E. *Introduction to Phase Transitions and Critical Phenomena*. (Oxford University Press, Oxford). (1987)
54. Zhao,L., Lai, Y.-C., Park, K., Ye, N. Onset of traffic congestion in complex networks. *Phys. Rev. E* 71:026125. (2005)